

## General Disclaimer

### One or more of the Following Statements may affect this Document

- This document has been reproduced from the best copy furnished by the organizational source. It is being released in the interest of making available as much information as possible.
- This document may contain data, which exceeds the sheet parameters. It was furnished in this condition by the organizational source and is the best copy available.
- This document may contain tone-on-tone or color graphs, charts and/or pictures, which have been reproduced in black and white.
- This document is paginated as submitted by the original source.
- Portions of this document are not fully legible due to the historical nature of some of the material. However, it is the best reproduction available from the original submission.

RADIATIVE INTERACTIONS OF  
ELECTRONS WITH MATTER

FINAL REPORT

Contract Number: NAS 8-24658

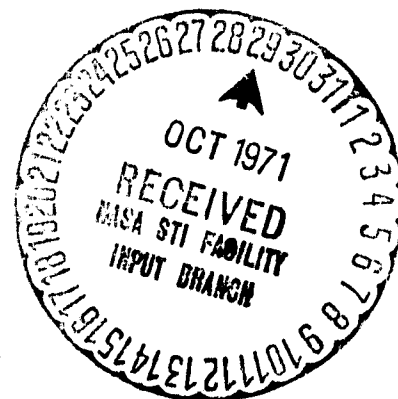
Prepared for George C. Marshall Space Flight Center,  
Marshall Space Flight Center, Alabama 35812

by

C. A. Quarles

Texas Christian University

Fort Worth, Texas 76129



September 1971

FACILITY FORM 602

N71-38368  
(ACCESSION NUMBER)

34  
(PAGES)

CR-719957  
(NASA CR OR TMX OR AD NUMBER)

\_\_\_\_\_  
(THRU)

53  
(CODE)

24  
(CATEGORY)

## INTRODUCTION

This is the final report on the work carried out in the Accelerator Laboratory at Texas Christian University under NASA Contract NAS 8-24658. The primary purpose of the basic research carried out under this Contract was to develop the necessary experimental techniques and to apply them to the study of various interactions of electrons with matter. During the period of the Contract, sophisticated experimental techniques have been developed and applied to the study of inner shell ionization by electrons, bremsstrahlung production by electrons, and electron scattering from a wide variety of targets in the energy range up to 140 keV. Since the research initiated under this Contract is, like all basic research, an ongoing thing; this report although it represents the final report on the work completed under this Contract, is more in the nature of an interim report of work in progress.

In what follows, Section I describes the present state of the experimental equipment and the research capabilities we have developed. Section II describes the experiments performed and presents the current state of the results of the work performed under this Contract. Section III lists the dissertations and publications resulting or expected from the work initiated or completed under this Contract. Section IV lists the personnel involved in the work supported by this Contract.

### I. EXPERIMENTAL EQUIPMENT AND CAPABILITY.

#### A. Beam

The electron beam is provided by a 150 keV linear accelerator which was converted from a Texas Nuclear 150 kV Cockcroft-Walton neutron generator. The

electron source is a commercially available electron gun. Several guns have been used including RCA 8520A, RCA 8714, and Griffith GE50 with essentially equivalent success. The beam is very stable over extended periods of time and is typically collimated to a 1/32 inch spot size at the target and operated at about  $10^{-8}$  amps. The beam is steered by a pair of Helmholtz coils and the only focussing used is that in the electron gun itself. The high voltage is variable from 20 to 150 keV and could probably be run at lower voltage if desired. The high voltage supply is filtered and the ripple is less than 0.01%. The beam tube, scattering chamber and Faraday Cup can be accurately aligned using a He-Ne laser beam. The beam tube is magnetically shielded and the targets and detectors are well shielded by lead from the radiation produced in the collimators along the beam tube. The electron beam-scattering chamber system we have developed is certainly one of the best and perhaps the best system available for the study of the various electron interactions in the keV energy range.

#### B. Scattering Chamber

The scattering chamber is a 12 inch chamber with ports at 0, 15, 30, 45, 60, 90, 135 and 270 degrees. The ports can be plugged or a detector can be positioned at any port and view the target through a 2.5 to 10 mil Mylar window. The target holder has three positions which can be remotely controlled. There is a moveable arm in the chamber to which Si(Li) electron detectors, or electron spectrometers can be mounted and remotely rotated to any desired angle. The chamber has two lids, one of which accepts a Ge(Li) photon detector which was especially designed to fit into the chamber. The chamber is mounted on a rigid frame and connected to the accelerator beam tube through a bellows. At

the entrance to the chamber is a tee which allows a 4 inch oil diffusion pump to be connected to the system. A Faraday Cup is usually placed at the exit of the scattering chamber to measure the beam current.

### C. Detectors

The laboratory has three major photon detectors: One Ge(Li) detector, 5 mm thick with a 10 mil Be window, which mounts in the scattering chamber lid; one Ge(Li) detector of the horizontal dipstick variety, 5 mm thick with a 5 mil Be window; and one Si(Li) X-ray detector, a horizontal dipstick model with a 1 mil Be window. The detectors complement each other and allow us to investigate with good efficiency the full photon energy range from about 3 keV to 150 keV. The efficiencies of these detectors have been accurately measured using calibrated radioactive sources. The energies and errors of the X-rays and gamma rays useful for calibration in our energy range are listed in Table 1 along with the measured absolute intensities. The sources and their half lives are listed in Table 2. The efficiency versus energy curves for the Si(Li) and the Ge(Li) detectors are given in Tables 3 and 4 and shown in Figures 1 and 2 respectively. The points for the Si(Li) detector are relative, but can be normalized to the absolute efficiency of  $(72 \pm 3.5)\%$  at 22.6 keV.

We have the electronics necessary to do single parameter pulse height analysis and two channel coincidence experiments with timing resolution of the order of 50 nsec. Of particular note is the magnetic tape readout system on our pulse height analyzer which greatly facilitates data handling and computer analysis.

### D. Targets

We have developed the capability of making thin targets by vacuum evap-

oration techniques and of accurately determining their thickness by direct weighing on a Cahn electrobalance. Of particular interest is the capability of making thin carbon targets (5 to 15  $\mu\text{g}/\text{cm}^2$ ) which can be used as backings for the evaporation of thin metallic targets. We have made numerous self supporting and carbon-backed targets of aluminum, copper, silver, and gold with thicknesses exceeding about 30  $\mu\text{g}/\text{cm}^2$ . In addition we have made thin targets ( $<200 \mu\text{g}/\text{cm}^2$ ) of rare earth oxides ( $57 \leq Z \leq 70$ ) on thin Vyns film backing.

## II. EXPERIMENTAL RESULTS.

### A. K-Shell Ionization Cross Section Measurements.

Absolute total cross sections for K-shell ionization have been measured for copper from 20 keV to 135 keV, for silver from 30 keV to 140 keV, and for gold from 90 keV to 140 keV. The results are given in Table 5. In addition to the run dependent errors, there are listed additional systematic errors in Table 6. A full discussion of the experiment and data analysis is contained in the Ph.D. dissertation submitted to T.C.U. by Mr. Doyle V. Davis which, due to its length, will not be included in this report.

The results are presented graphically in Figures 3, 4, and 5 where comparison with the experiments of Motz and Placious<sup>7</sup>, Rester and Dance<sup>8</sup>, Fischer and Hoffman<sup>9</sup>, and Hansen et al<sup>10</sup> and with the theoretical work of Arthurs and Moiseivitch (AM)<sup>1</sup>, Gryzinski<sup>2</sup> and Kolbenstvedt<sup>3</sup> is made. The agreement among experiments is generally within the systematic errors except for the data of Hansen et al<sup>10</sup>, which seems to disagree with other work especially at higher energies. Except very near the threshold, the theory of Kolbenstvedt is in good agreement with our data. The agreement with AM appears good for silver, but

this agreement may be fortuitous since the agreement with copper is not very good. The theory of AM also does not agree very well with recent aluminum data of Hink and Ziegler<sup>4</sup>. The agreement with Gryzinski's classical theory is certainly as good as that with the AM quantum mechanical calculation as far as shape is concerned. Increasing the Gryzinski prediction by about 20 to 25% would bring it into good agreement with the experiment<sup>4</sup>. This, we feel, is a very interesting result and suggests that as good an estimate of the K ionization cross section may be provided by Gryzinski's or Kolbenstvedt's calculation as by that of AM. In no case, however, is the agreement between theory and experiment completely satisfactory. More experimental work in this field is certainly called for to resolve these difficulties. We hope to undertake a more complete study in this energy range for a wide variety of atomic numbers.

#### B. L-Shell Ionization Cross Section Measurements.

Absolute total cross sections for the  $L_{III}$ - shell ionization of gold have been measured from 30 keV to 140 keV. The results are presented in Table 7. The additional systematic errors are shown in Table 8. The data are presented graphically in Figure 6 where comparison can be made with the theory of Gryzinski and Kolbenstvedt. Again, agreement is not bad although the theoretical curves lie below the measurements in both cases.

The work on K-shell and L-shell ionization is being prepared for publication in Physical Review. While further analysis of the data is underway, it is not expected to systematically alter the results given here. The analysis of the errors will be refined and some multiple scattering corrections will be made which affect the lower energies somewhat. The work adds considerably to our

knowledge in this important field and clearly points out the need for further precise experimental work for a wider range of atomic numbers as well as more theoretical work, especially near threshold.

### C. X-Ray Intensity Ratios.

$K_{\alpha}/K_{\beta}$  X-ray intensity ratios have been measured for a variety of atomic numbers. The results have been published in Nuclear Physics A164, 219 (1971) and in Physics Letters A (to be published) and are presented in Table 9 and graphically in Figure 7. In the figure, comparison is made with other experiments and with the calculations of Scofield<sup>5</sup> and Rosner and Bhalla<sup>6</sup>. The ratio for copper has been measured with the Si(Li) detector and the error in this point reflects the great improvement which results from the better resolution of the Si(Li) detector. Clearly, a sensitive test of the calculations could be made for atomic numbers in the  $24 < Z < 32$  region and we intend to undertake these further measurements. Over the range measured, the theory is systematically higher than the experiments. Agreement between experiments is generally good except for low Z where our results disagree with the work of Ebert and Slivinsky<sup>11</sup>.

### D. Bremsstrahlung Spectrum Measurements.

Extensive data has been and is being taken on the bremsstrahlung interaction. Incident electron energies of 50, 100, and 140 keV, photon emission angles of 30, 45, 60, 90, and 135 degrees, and targets of carbon, aluminum, copper, silver, and gold have been investigated. The analysis of the data is still in process and these results should form a part of the Ph.D. dissertation to be submitted to T.C.U. by Mr. David Heroy. Some typical bremsstrahlung spectra, plotted by the IBM 1800 computer from some of our data tapes, showing



both target in and target out runs are in Figures 8 through 16. It can be seen that the end point of the spectrum is well resolved and that the background is not excessive. The peak in the background, visible at 140 keV in the Ag and Au data (Figures 13 and 16), has been removed by increasing shielding as shown in the Al data (Figure 10) taken subsequently. Analysis of these spectra is underway, and involves folding in efficiency and calibration runs as well as normalization to total incident charge before precise cross sections can be given. These results should provide new extensive experimental information for critical comparison with the existing calculations and with other experiments.

#### E. Inelastic Electron Scattering.

The work done on inelastic electron scattering and the essential conclusion that the amount of inelastic scattering we can measure in our energy range is not significant has been summarized in the November 1970 quarterly progress report, and will not be repeated here. We are still, however, interested in a study of Møller scattering and believe we should be able to obtain some significant results on this process with our present apparatus.

#### F. Coincidence Experiments.

The results obtained on the measurement of the coincidence between the inelastically scattered electron and bremsstrahlung are reproduced in Figure 18. These results have been discussed in the February 1971 quarterly progress report. They were made at 140 keV incident electron energy and photon angle  $270^\circ$  from a  $165 \mu\text{g}/\text{cm}^2$  silver target. Rather than simply run for additional statistics on these points, we felt that better electron energy and angular resolution were still needed. Hence, we have designed and built a new electrostatic electron spectrometer. This spectrometer, while similar in design to the previous one,

is designed to bend the electrons through  $120^\circ$  in the horizontal plane. The angular resolution is thus considerably improved and the energy resolution also looks significantly better than that of the old spectrometer. As yet, however, no additional coincidence data has been taken using this spectrometer. One further remark concerns the timing resolution. We are able to get about 50 nsec resolving time with our present electronics. The state of the art of timing with solid state detectors has now improved to the extent that we could perhaps gain a factor of 5 to 10 in resolving time by using a Canberra Extrapolated Zero Strobe timing circuit on each coincidence channel. Such a gain would improve the true coincidence to accidental rate by about this factor and certainly make the coincidence count rate significantly easier to detect.

We have not been able with our system to detect coincidences between electrons and K X-rays since the expected cross section appears to be well below the present sensitivity of our apparatus.

While much work remains to be done with coincidence measurements, we believe that we have made a significant advance in elucidating the experimental difficulties involved in such measurements. We will continue work in this important field and expect that significant results will be presented as a Ph.D. dissertation by Mr. Jerry Faulk.

### III. PUBLICATIONS.

The following publications, apart from the quarterly progress reports, have resulted from the work supported by this contract:

1. Inelastic Electron - Atom Interactions from 50 to 150 keV, Proceedings of the Second Conference on the Use of Small Accelerators for Teaching and Research, USAEC - Conf 700322, p.379 (1970).

2.  $K_{\alpha}/K_{\beta}$  X-ray Intensity Ratios from Electron Bombardment, Bull. Am. Phys. Soc. 15, 1304 (1970); and Nuclear Physics A164, 219 (1971).
3. Measurement of Inner Shell Ionization Cross Sections for Cu, Ag, and Au; Bull. Am. Phys. Soc. 15, 1305 (1970).
4.  $K_{\alpha}/K_{\beta}$  X-ray Intensity Ratios for  $57 \leq Z \leq 70$  from Electron Bombardment. Bull. Am. Phys. Soc. 16, 546 (1971); and Physics Letters A (to be published).
5. Inner Shell Ionization of Copper, Silver, and Gold from Electron Bombardment; Ph.D. dissertation by D. V. Davis (1971), unpublished. Paper in preparation for submission for publication in Physical Review A. In addition, further publication can be expected from work in progress at this time which was begun under this contract.
6. Bremsstrahlung Cross Section Measurements at 50, 100, 140 keV From Carbon, Aluminum, Copper, Silver, and Gold; Ph.D. dissertation of D. Heroy expected January 1972, and associated publications.
7. Measurement of the Fundamental Bremsstrahlung Cross Section Differential in Photon Energy and Photon Electron Angles; expected Ph.D. dissertation of J. Faulk.

#### IV. PERSONNEL.

The work reported here was performed by the following people who have received direct financial support from this contract: Dr. C.A. Quarles, Principal Investigator; Dr. V.D. Mistry, postdoctoral fellow; Dr. D.V. Davis, graduate student; Mr. D. Heroy, graduate student; and Mr. J. Faulk, graduate student.

TABLE CAI IONS.

1. Energies and intensities of  $\gamma$ -rays and X-rays useful in efficiency measurements on solid state detectors from 4.5 to 166 keV.
2. Half lives and calibration accuracy of sources used in efficiency measurements.
3. Relative efficiency of Si(Li) detector.
4. Absolute efficiency of Ge(Li) detector.
5. K-shell ionization cross sections of copper, silver, and gold from 25 to 140 keV.
6. Systematic errors in K-shell ionization cross sections.
7.  $L_{III}$ -shell ionization cross section of gold from 20 to 140 keV.
8. Systematic errors in  $L_{III}$ -shell ionization cross sections.
9.  $K_{\alpha}/K_{\beta}$  X-ray intensity ratios for  $29 \leq Z \leq 79$ .

## REFERENCES

1. A.M. Arthurs and B.L. Moiseivitsch, Proc. Roy. Soc. (London) A247, 550 (1958).
2. M. Gryzinski, Phys. Rev. 138, A336 (1965).
3. M. Kolbenstvedt, J. Appl. Phys. 38, 4785 (1967).  
L.M. Middleman et al, Phys. Rev. A2, 1429 (1970).
4. W. Hink and A. Ziegler, Z. Physik 226, 222 (1969).
5. J. Scofield, Phys. Rev. 179, 9 (1969).
6. H.R. Rosner and C.P. Bhalla, Z. Physik 231, 347 (1970).
7. J.W. Motz and R.C. Placious, Phys. Rev. 136, A662 (1964).
8. D.M. Rester and W.E. Dance, Phys. Rev. 152, 1 (1966).
9. B. Fischer and K.W. Hoffman, Z. Physik 204, 122 (1967).
10. M. Hansen, H. Weigman, A. Flammersfeld, Nuc. Phys. 58, 241 (1969).
11. P.J. Ebert and V.W. Slivinsky, Phys. Rev. 188, 1 (1969);  
Phys. Letters 29A, 463 (1969).
12. J.S. Hansen, H.U. Freund, and R.W. Fink, Nuc. Phys. A142, 604 (1970).

TABLE I. ENERGIES AND INTENSITIES USED IN EFFICIENCY MEASUREMENT

Energy (keV)	Type of Radiation	Parent Nucleus	Intensity (Photons per 100 Disintegrations)
4.47	X <sub>L</sub>	<sup>137</sup> Cs	1.25 $\pm$ .01
5.95	X <sub>K</sub>	<sup>55</sup> Fe	25.7 $\pm$ .1
6.46	X <sub>K</sub>	<sup>57</sup> Co	54 $\pm$ 2
10.27	X <sub>L</sub>	<sup>203</sup> Hg	5.63 $\pm$ .08
11.887 $\pm$ .004	X <sub>L</sub>	<sup>241</sup> Am	0.80 $\pm$ .04
13.9 $\pm$ .1	X <sub>L<math>\alpha</math></sub>	<sup>241</sup> Am	13.50 $\pm$ .54
14.408 $\pm$ .005	$\gamma$	<sup>57</sup> Co	9.5 $\pm$ .2
17.8 $\pm$ .1	X <sub>L<math>\beta</math></sub>	<sup>241</sup> Am	18.40 $\pm$ .74
20.8 $\pm$ .1	X <sub>L<math>\gamma</math></sub>	<sup>241</sup> Am	5.0 $\pm$ .2
22.581	X <sub>K</sub>	<sup>109</sup> Cd	102 $\pm$ 4
26.35 $\pm$ .01	$\gamma$	<sup>241</sup> Am	2.5 $\pm$ .2
31.635	X <sub>K</sub>	<sup>133</sup> Ba	84.2 $\pm$ 9.0
32.88	X <sub>K</sub>	<sup>137</sup> Cs	6.88 $\pm$ .04
33.20 $\pm$ .01	$\gamma$	<sup>241</sup> Am	0.14 $\pm$ .04
34.169	X <sub>K</sub>	<sup>139</sup> Ce	81.5 $\pm$ 8.2
43.42 $\pm$ .02	$\gamma$	<sup>241</sup> Am	0.073 $\pm$ .007
53.18 $\pm$ .04	$\gamma$	<sup>133</sup> Ba	1.96 $\pm$ .22
55.54 $\pm$ .02	$\gamma$	<sup>241</sup> Am	0.020 $\pm$ .002
59.536 $\pm$ .001	$\gamma$	<sup>241</sup> Am	35.3 $\pm$ .5
74.60	X <sub>K</sub>	<sup>203</sup> Hg	12.8 $\pm$ .2
81.1 $\pm$ .3	$\gamma$	<sup>133</sup> Ba	33.5 $\pm$ 4.3
87.7 $\pm$ .2	$\gamma$	<sup>109</sup> Cd	3.91 $\pm$ .08
98.97 $\pm$ .03	$\gamma$	<sup>241</sup> Am	0.021 $\pm$ .002

Table I Cont.

103.0 $\pm$ .1	$\gamma$	$^{241}\text{Am}$	0.019 $\pm$ .002
103.48	$X_K$	$^{241}\text{Am}$	0.08 $\pm$ .02
122.07 $\pm$ .03	$\gamma$	$^{57}\text{Co}$	85.6 $\pm$ .2
136.43 $\pm$ .05	$\gamma$	$^{57}\text{Co}$	10.6 $\pm$ .2
160.66 $\pm$ .06	$\gamma$	$^{133}\text{Ba}$	0.626 $\pm$ .074
165.84 $\pm$ .03	$\gamma$	$^{139}\text{Ce}$	79.91 $\pm$ .07

TABLE 2. HALF-LIVES OF SOURCES USED IN EFFICIENCY MEASUREMENT

Source	Half-life	Calibration Uncertainty <sup>a</sup>
$^{55}\text{Fe}$	2.7 $\pm$ .1 y	3.8%
$^{57}\text{Co}$	270 $\pm$ 2 d	2.2%
$^{109}\text{Cd}$	462.6 $\pm$ .4 d	1.4%
$^{133}\text{Ba}$	10.66 $\pm$ .12 y	2.8%
$^{137}\text{Cs}$	30.0 $\pm$ .5 y	2.9%
$^{139}\text{Ce}$	137.50 $\pm$ .30 d	2.3%
$^{203}\text{Hg}$	46.59 $\pm$ .05 d	1.7%
$^{241}\text{Am}$	433 $\pm$ 2 y	1.9%

<sup>a</sup> Represents one standard deviation.

Table 3. Relative Efficiency Data for Si(Li).

<u>Energy (keV)</u>	<u>Efficiency (%)</u>
4.47	47.9 + 2.3
5.95	66.3 - 4.2
6.46	75.0 3.9
11.8	65.0 2.3
11.9	74.7 4.4
14.4	77.1 2.7
13.9	70.4 3.3
17.8	70.5 3.3
20.8	55.5 2.6
26.4	39.0 1.8
22.6	55.7 1.7
32.9	30.9 1.0
34.2	23.5 2.5
59.5	4.59 .12
74.6	2.29 .07
88.0	1.61 .03

Absolute Efficiency at 22.6 keV is 72<sub>-</sub>3.5

Table 4. Absolute Efficiency Data for Ge(Li).

<u>Energy (keV)</u>	<u>Efficiency (%)</u>
5.95	61.4 + 4.8
6.46	63.4 - 3.6
10.27	60.6 2.7
14.4	69.6 2.8
13.9	70.2 4.5
17.8	74.2 4.1
20.8	75.0 3.9
22.6	76.9 3.1
26.4	84.0 7.3
32.9	95.5 3.7
34.2	93.3 9.8
43.4	87.4 9.3
59.5	95.0 3.1
74.6	90.7 3.2
87.7	74.9 1.8
122.1	45.7 1.5
136.4	36.6 1.6
165.8	23.0 .8



Table 5. K-shell Ionization Cross Sections.

<u>Energy (keV)</u>	<u>Cu (barns)</u>	<u>Ag (barns)</u>	<u>Au (barns)</u>
25	450 $\pm$ 7		
30	477 $\pm$ 6	26.0 $\pm$ 0.6	
40	445 $\pm$ 4	50.4 $\pm$ 0.9	
50		63.9 $\pm$ 1.0	
60	428 $\pm$ 13	68.7 $\pm$ 1.1	
80	391 $\pm$ 3	68.6 $\pm$ 0.7	
90			2.5 $\pm$ 0.3
100	325 $\pm$ 4	69.6 $\pm$ 0.6	4.5 $\pm$ 0.1
120		68.4 $\pm$ 0.7	6.0 $\pm$ 0.1
135	299 $\pm$ 2		
140		66.1 $\pm$ 1.0	6.6 $\pm$ 0.1

Table 6. Percent Systematic Errors in K-shell Ionization Cross Sections.

<u>Error Source</u>	<u>Cu (%)</u>	<u>Ag (%)</u>	<u>Au (%)</u>
Solid angle	2.5	2.5	2.5
Detector efficiency	5.0	5.0	5.0
Fluorescence yield	2.9	2.3	3.0
Target angle	2.0	2.0	2.0
Faraday cup efficiency	5.0	5.0	5.0
Target thickness	20.0	5.0	5.0
Total	22.0%	9.5%	9.7%

Table 7. Gold L<sub>III</sub>-shell Ionization Cross Sections.

<u>Energy (keV)</u>	<u>AuL<sub>III</sub> (barns)</u>
20	702 + 84
25	690 + 35
30	706 + 7
40	695 + 8
60	643 + 7
80	552 + 12
100	509 + 16
120	460 + 6
140	450 + 7

Table 8. Percent Systematic Errors in L<sub>III</sub> Ionization Cross Sections.

<u>Error Source</u>	<u>Au (%)</u>
Solid angle	2.5
Detector efficiency	5.0
Fluorescence yield	9.4
Target angle	2.0
Faraday cup efficiency	5.0
Target thickness	5.0
Total	13.0%

Table 9.  $K_{\alpha}/K_{\beta}$  X-ray Intensity Ratios.

<u>Z</u>	<u><math>K_{\alpha}/K_{\beta}</math></u>
29	7.88 + .11
30	7.52 + .45
47	4.72 + .09
50	4.68 + .09
57	4.26 + .08
58	4.02 + .08
59	4.04 + .08
60	4.14 + .10
64	3.88 + .09
66	3.79 + .08
67	3.92 + .08
68	3.94 + .10
70	3.70 + .08
79	3.63 + .25

## FIGURE CAPTIONS.

1. Relative efficiency of Si(Li) detector.
2. Absolute efficiency of Ge(Li) detector,
3. Copper K-shell ionization cross section versus incident electron energy.
4. Silver K-shell ionization cross section versus incident electron energy.
5. Gold K-shell ionization cross section versus incident electron energy.
6. Gold  $L_{III}$ -shell ionization cross section versus incident electron energy.
7.  $K_{\alpha}/K_{\beta}$  X-ray intensity ratios versus atomic number.
8. Bremsstrahlung spectrum at  $60^{\circ}$  for 50 keV electrons on aluminum.
9. Bremsstrahlung spectrum at  $60^{\circ}$  for 100 keV electrons on aluminum.
10. Bremsstrahlung spectrum at  $60^{\circ}$  for 140 keV electrons on aluminum.
11. Bremsstrahlung spectrum at  $60^{\circ}$  for 50 keV electrons on gold.
12. Bremsstrahlung spectrum at  $60^{\circ}$  for 100 keV electrons on gold.
13. Bremsstrahlung spectrum at  $60^{\circ}$  for 140 keV electrons on gold.
14. Bremsstrahlung spectrum at  $45^{\circ}$  for 50 keV electrons on silver.
15. Bremsstrahlung spectrum at  $45^{\circ}$  for 100 keV electrons on silver.
16. Bremsstrahlung spectrum at  $45^{\circ}$  for 140 keV electrons on silver.
17. Bremsstrahlung cross section differential in photon energy, photon angle and electron angle versus photon energy at  $\theta_{\gamma}$  of  $270^{\circ}$  for 140 keV electrons on silver.

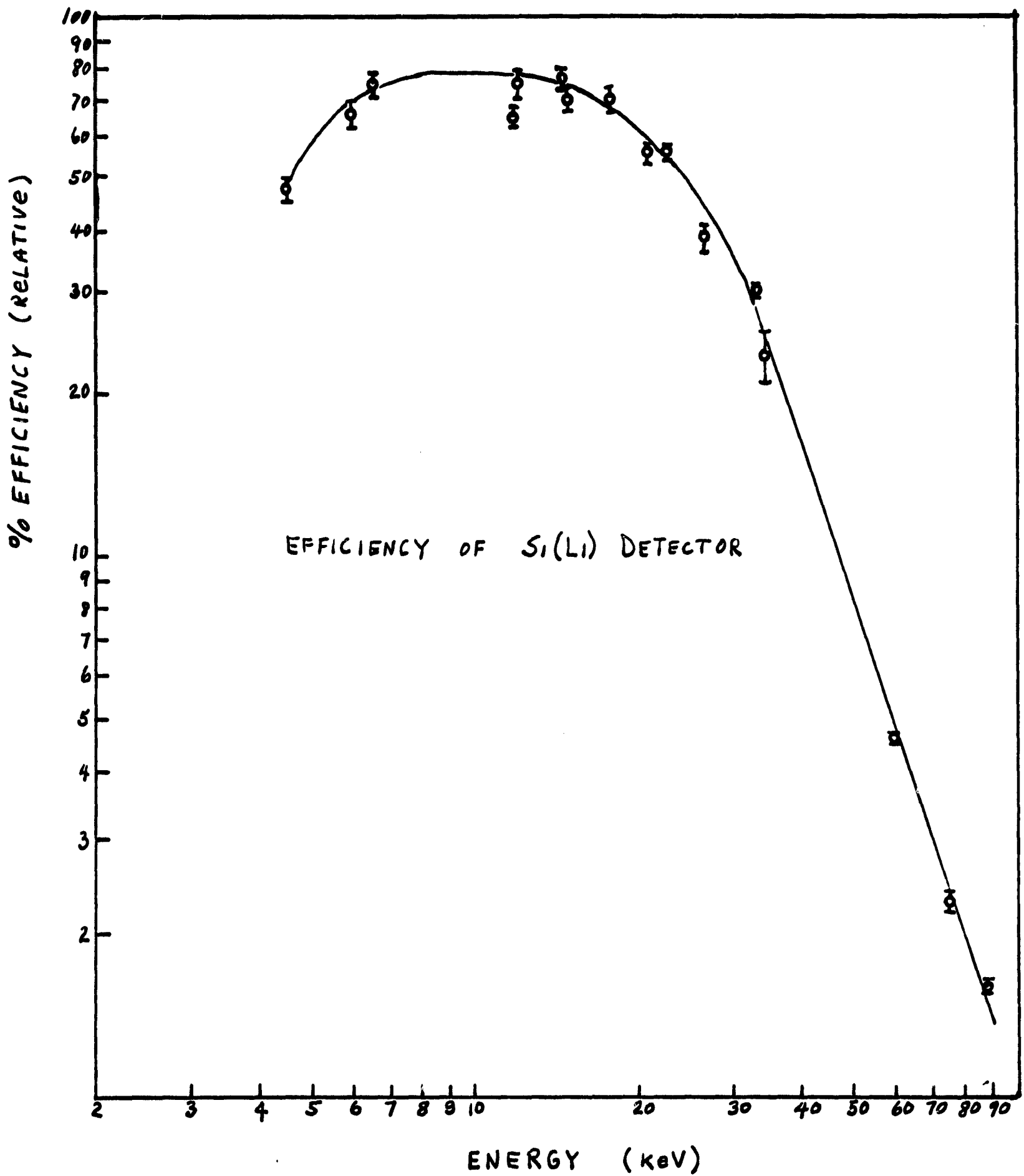


FIG. 1

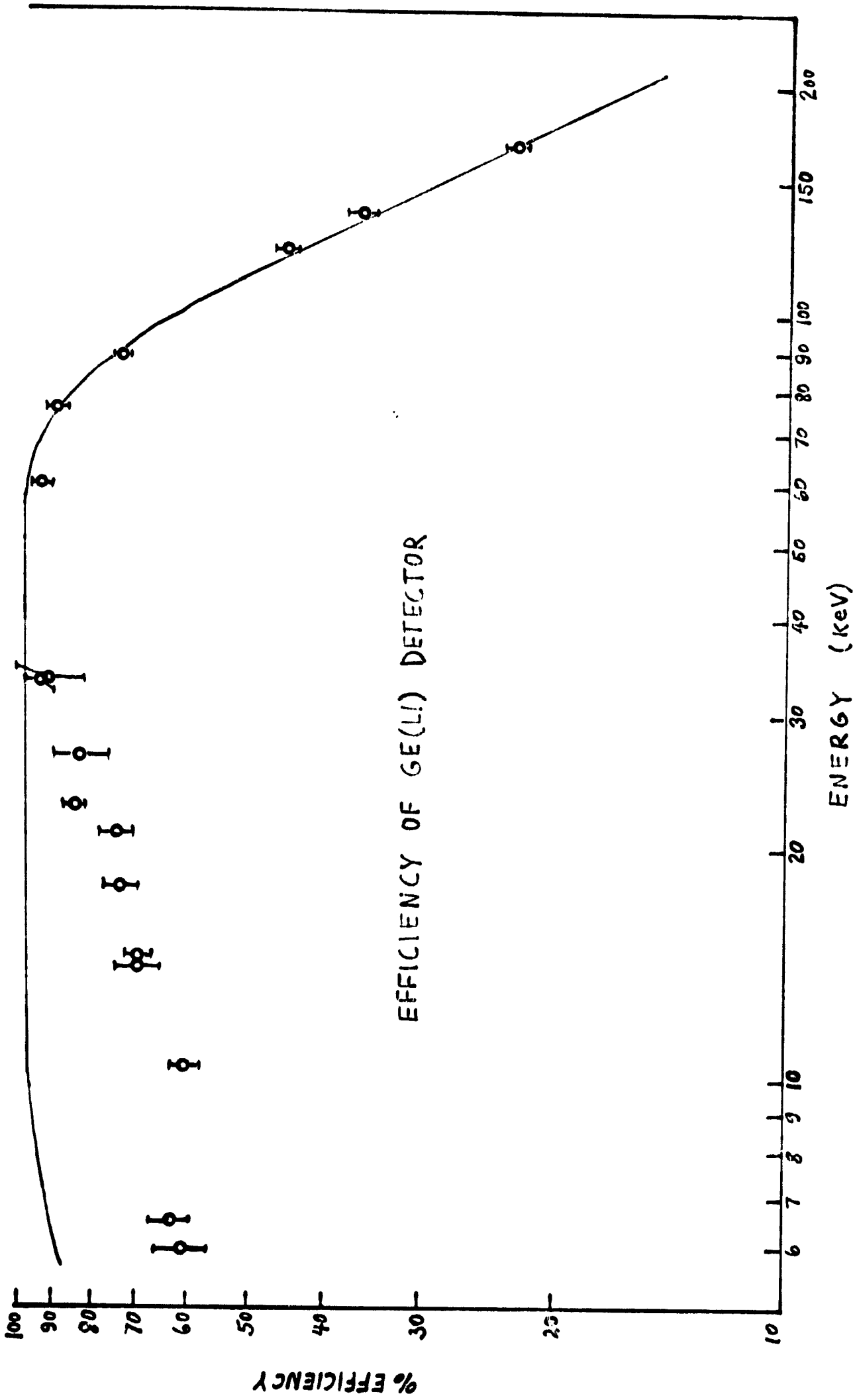


FIG. 2

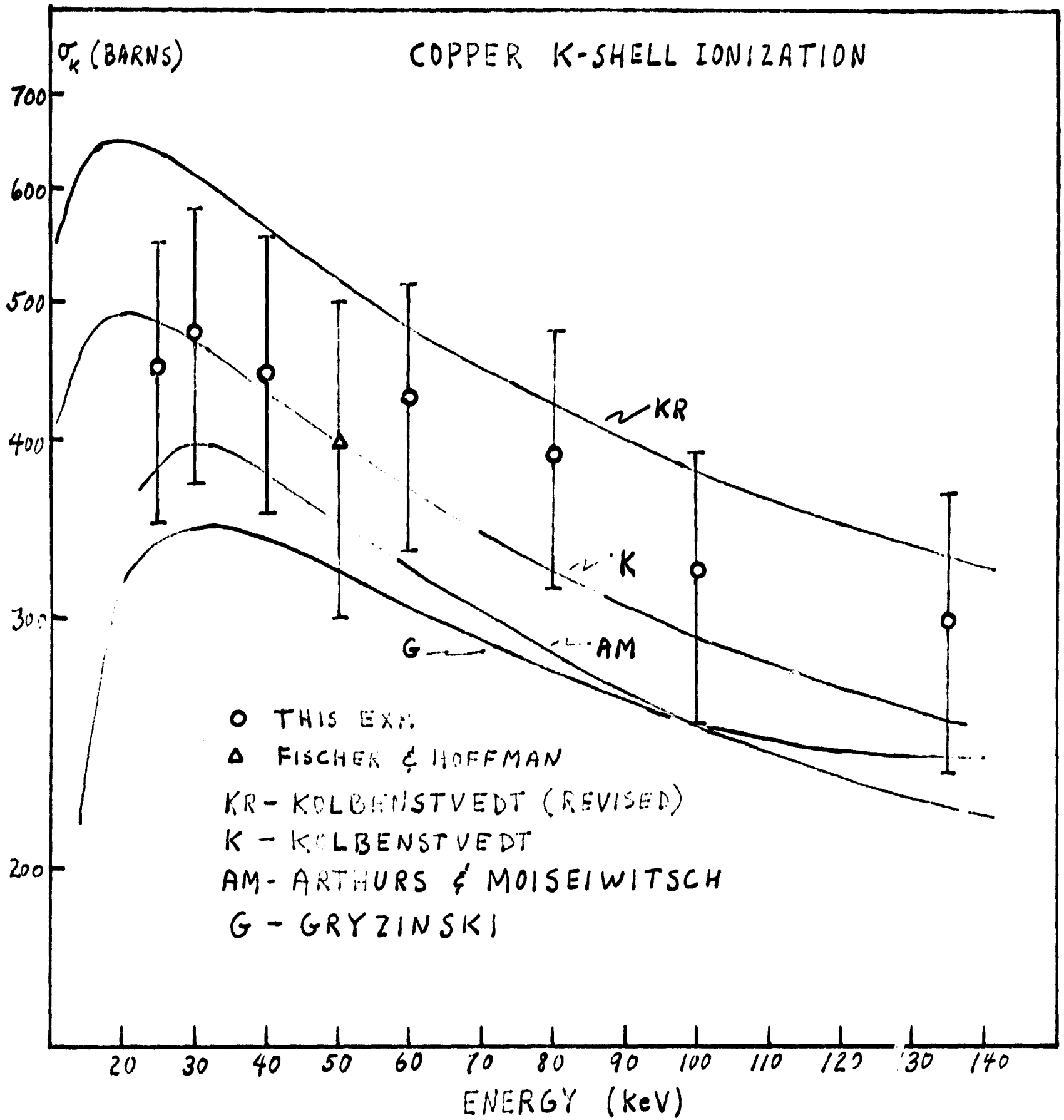


FIG. 3

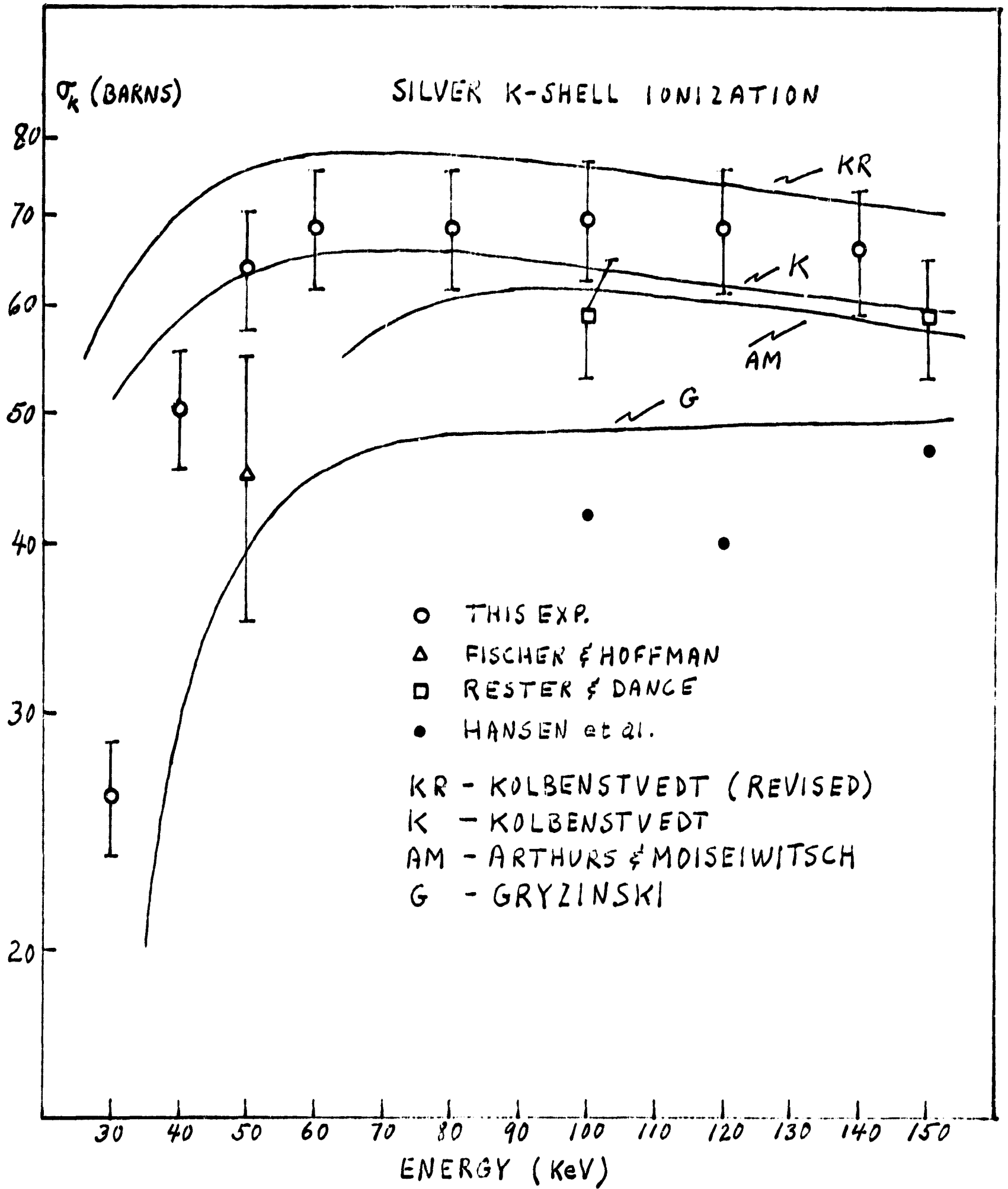


FIG. 4

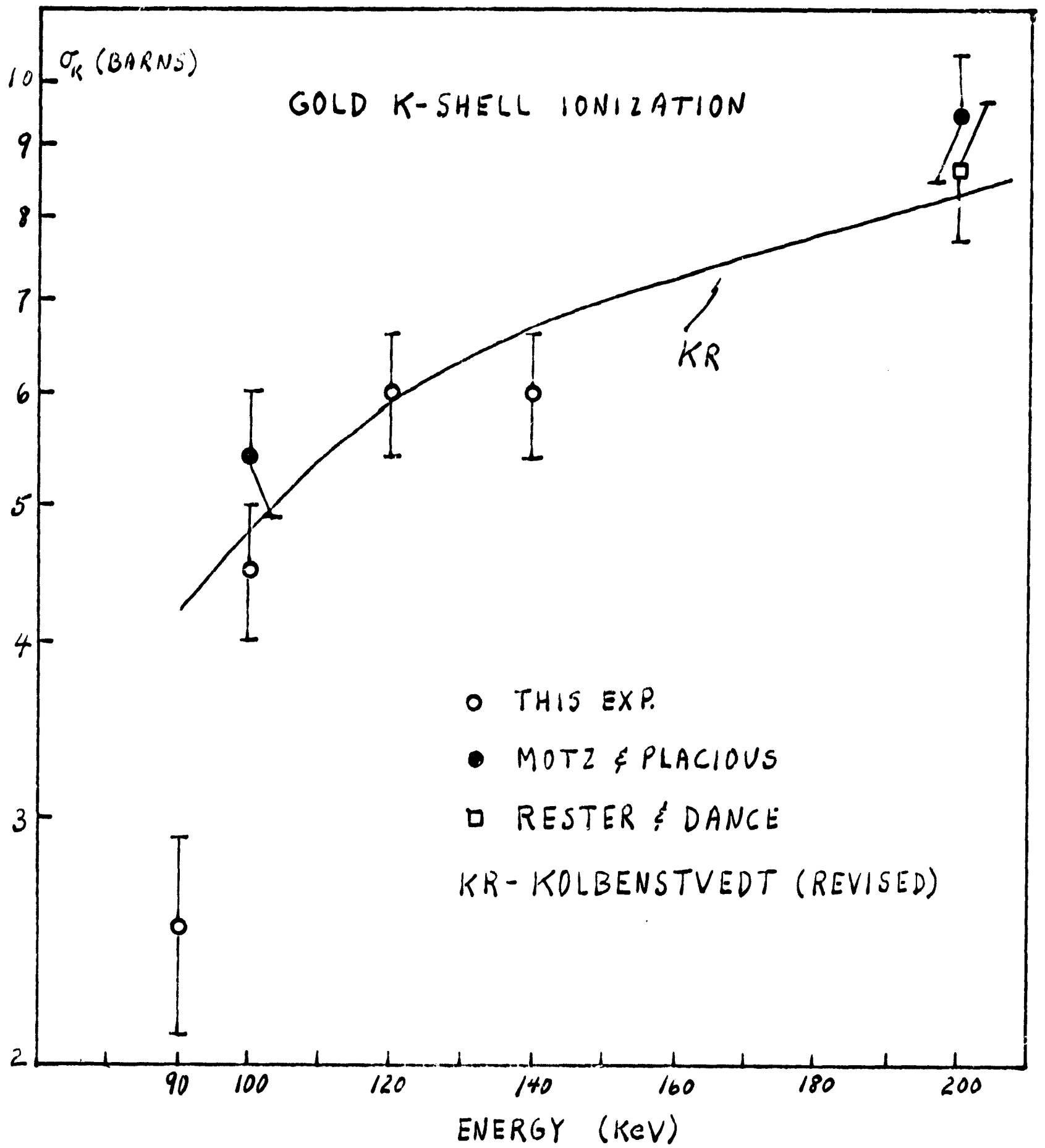


FIG. 5



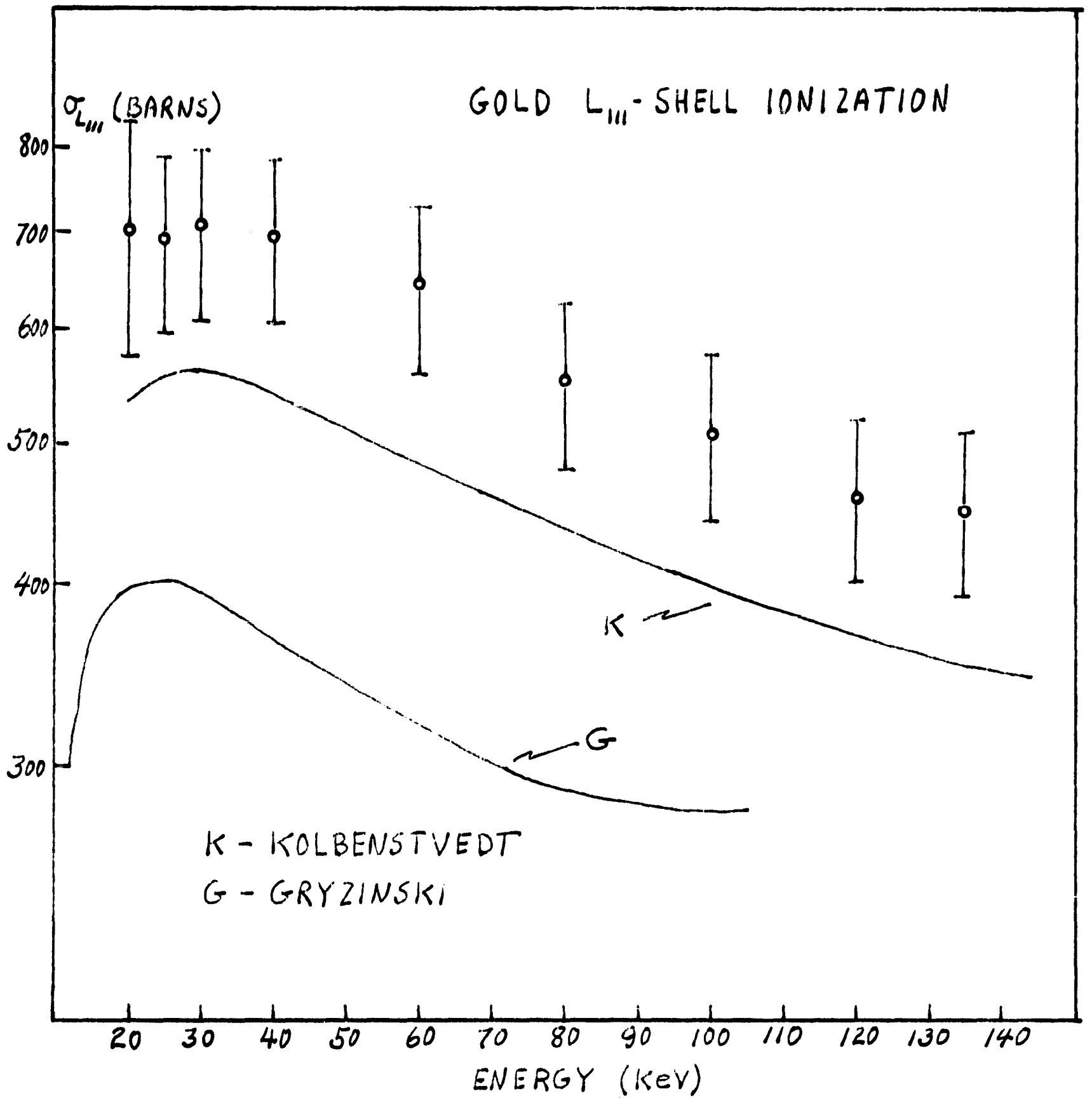


FIG. 6

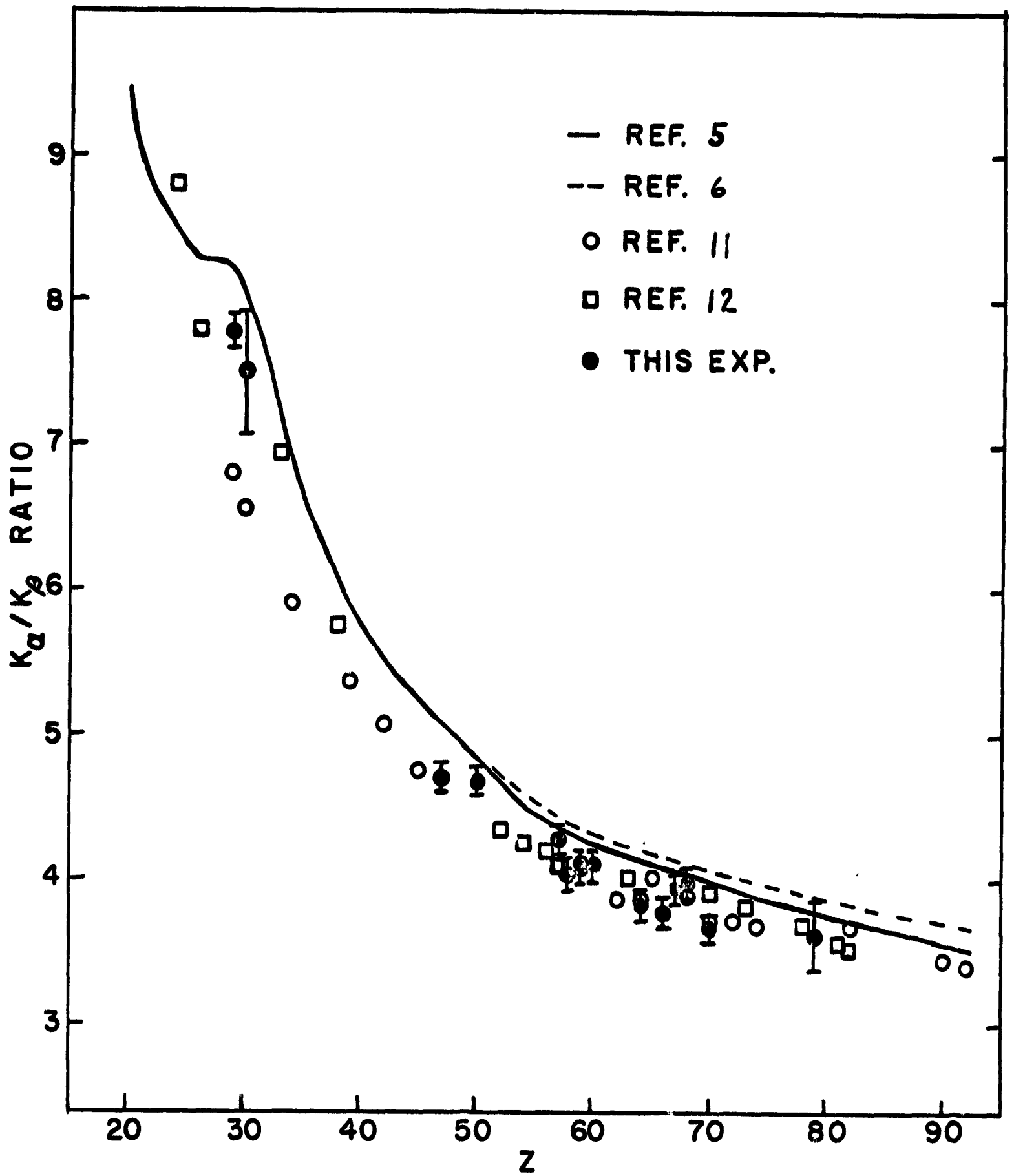


FIG. 7

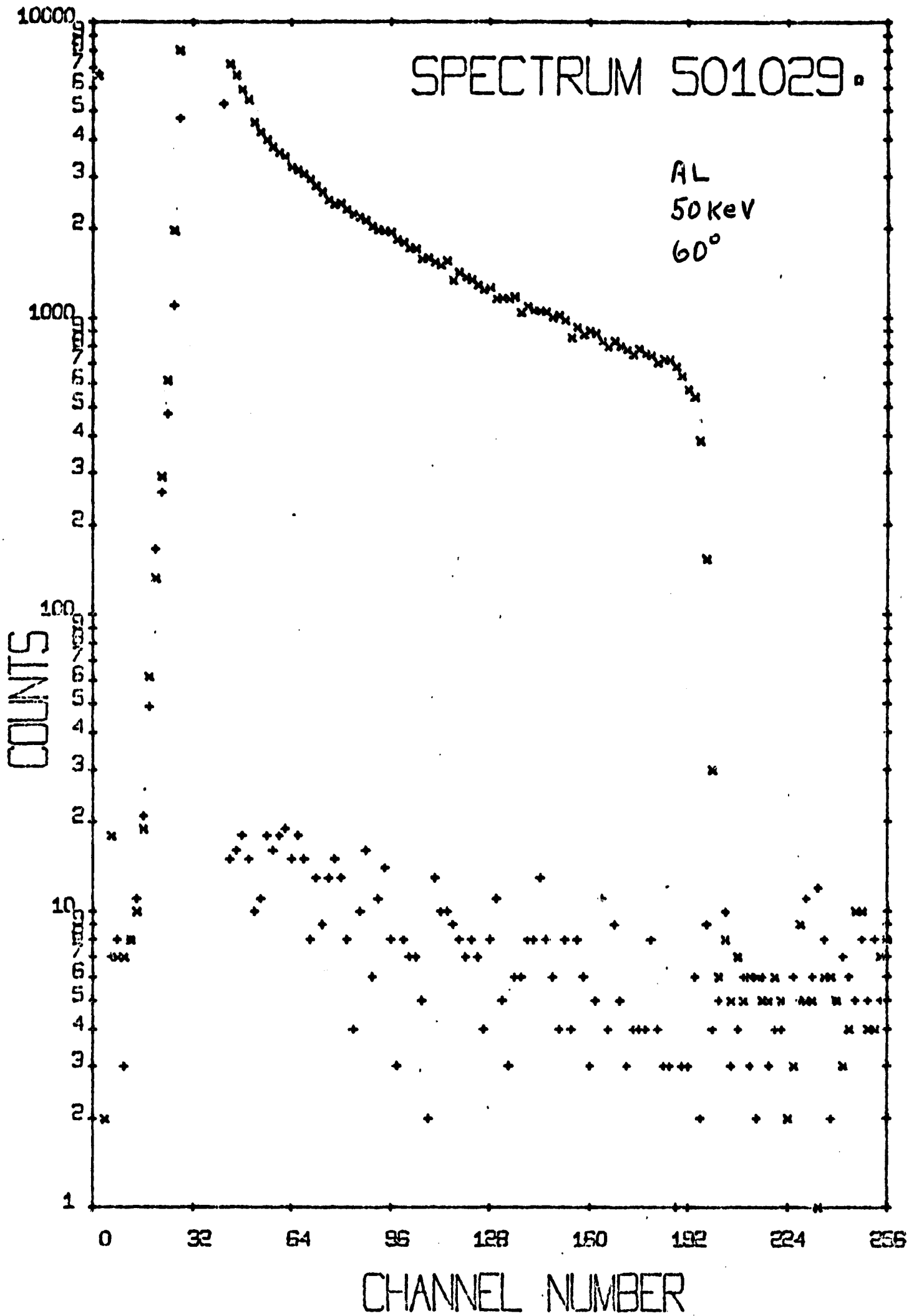


FIG. 8

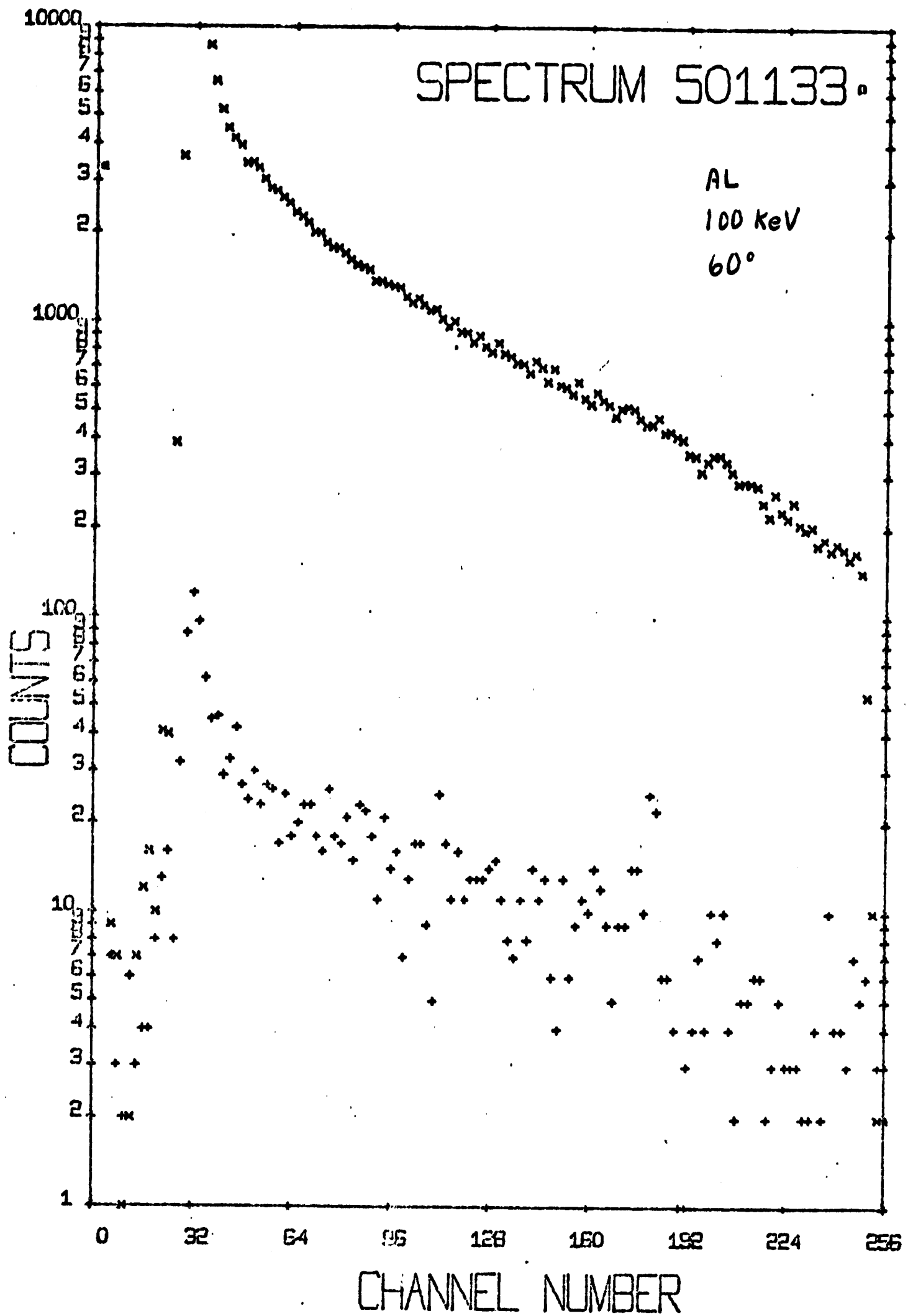


FIG. 9

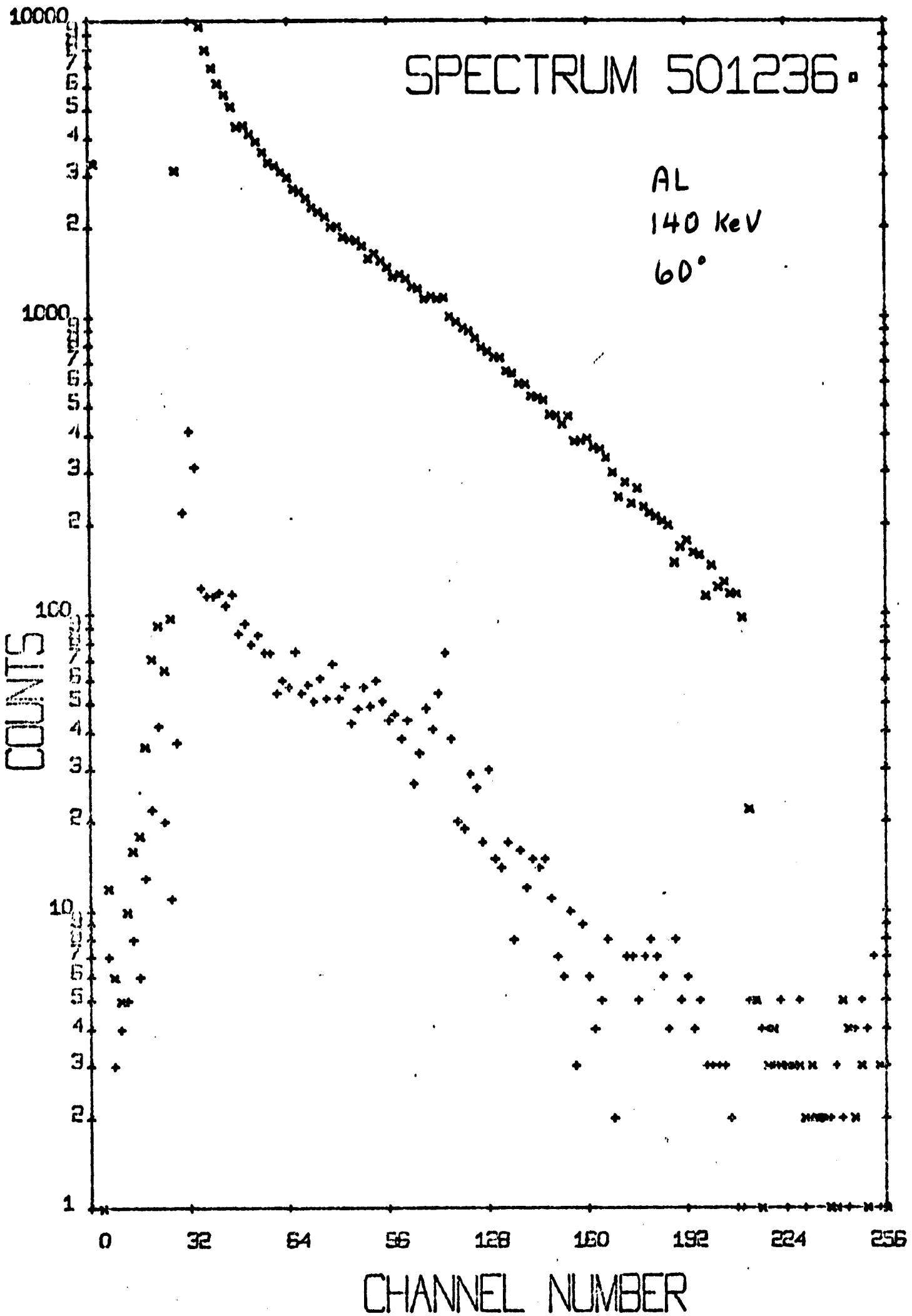


FIG. 10

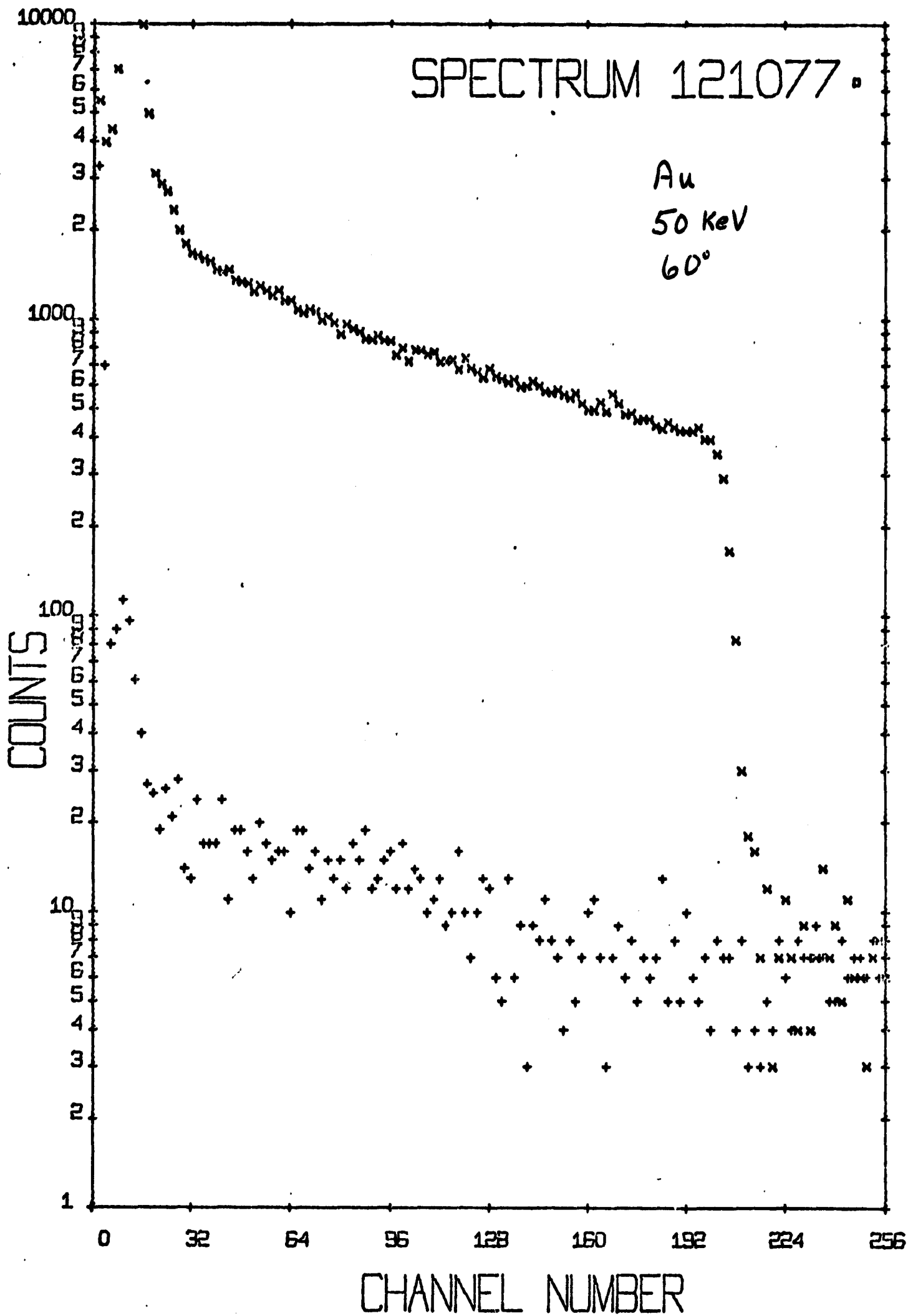


FIG. 11

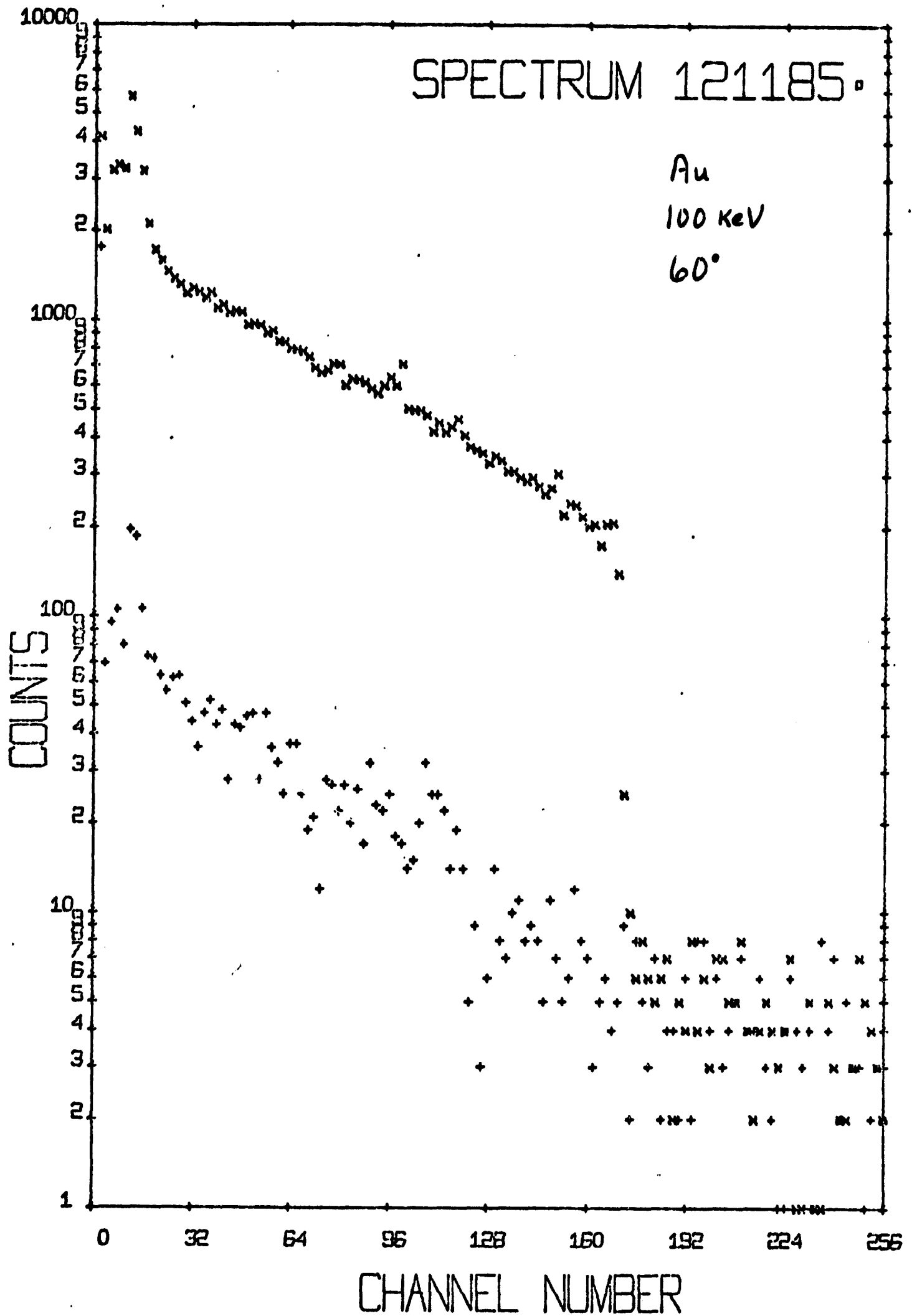


FIG. 12

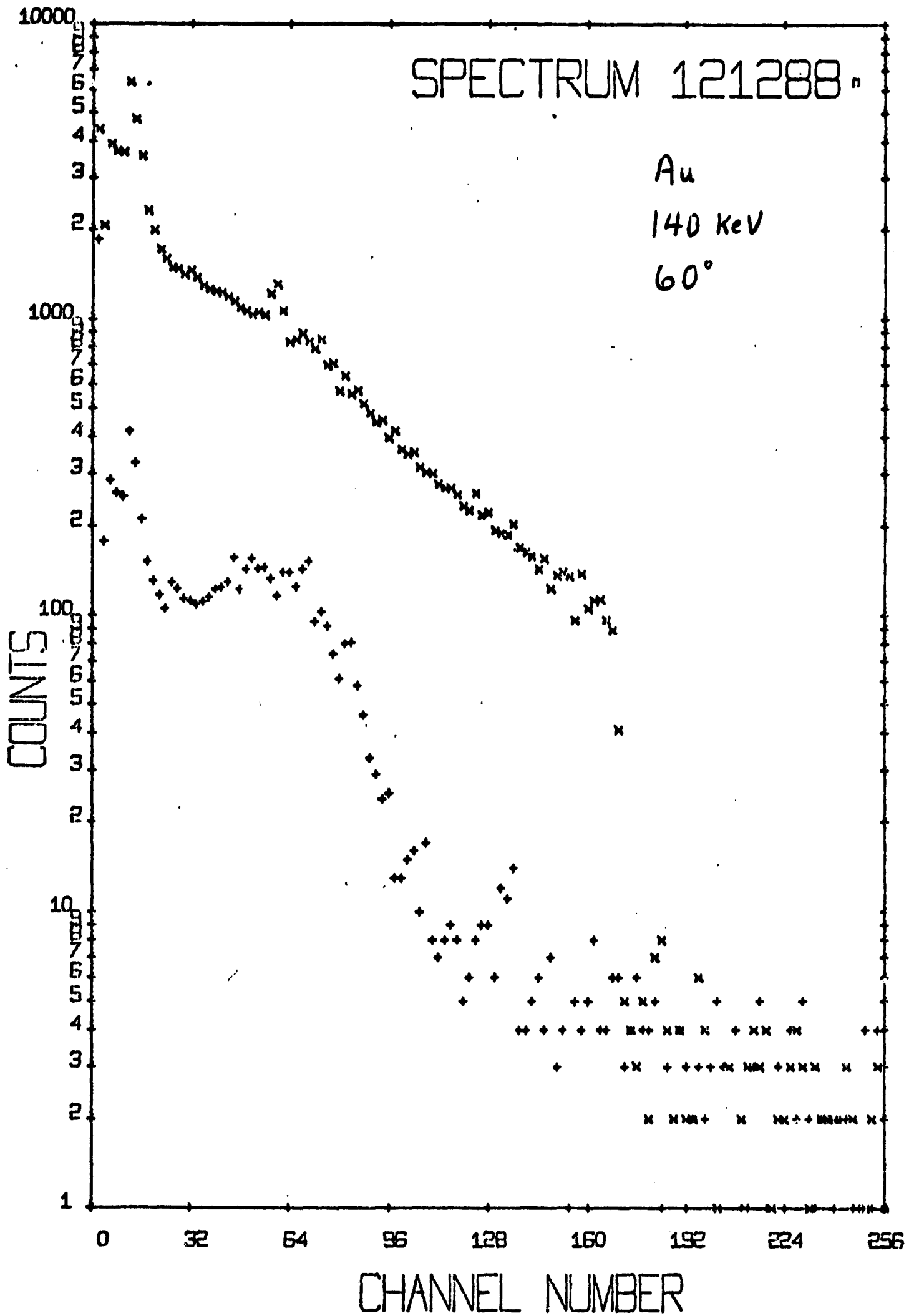


FIG. 13



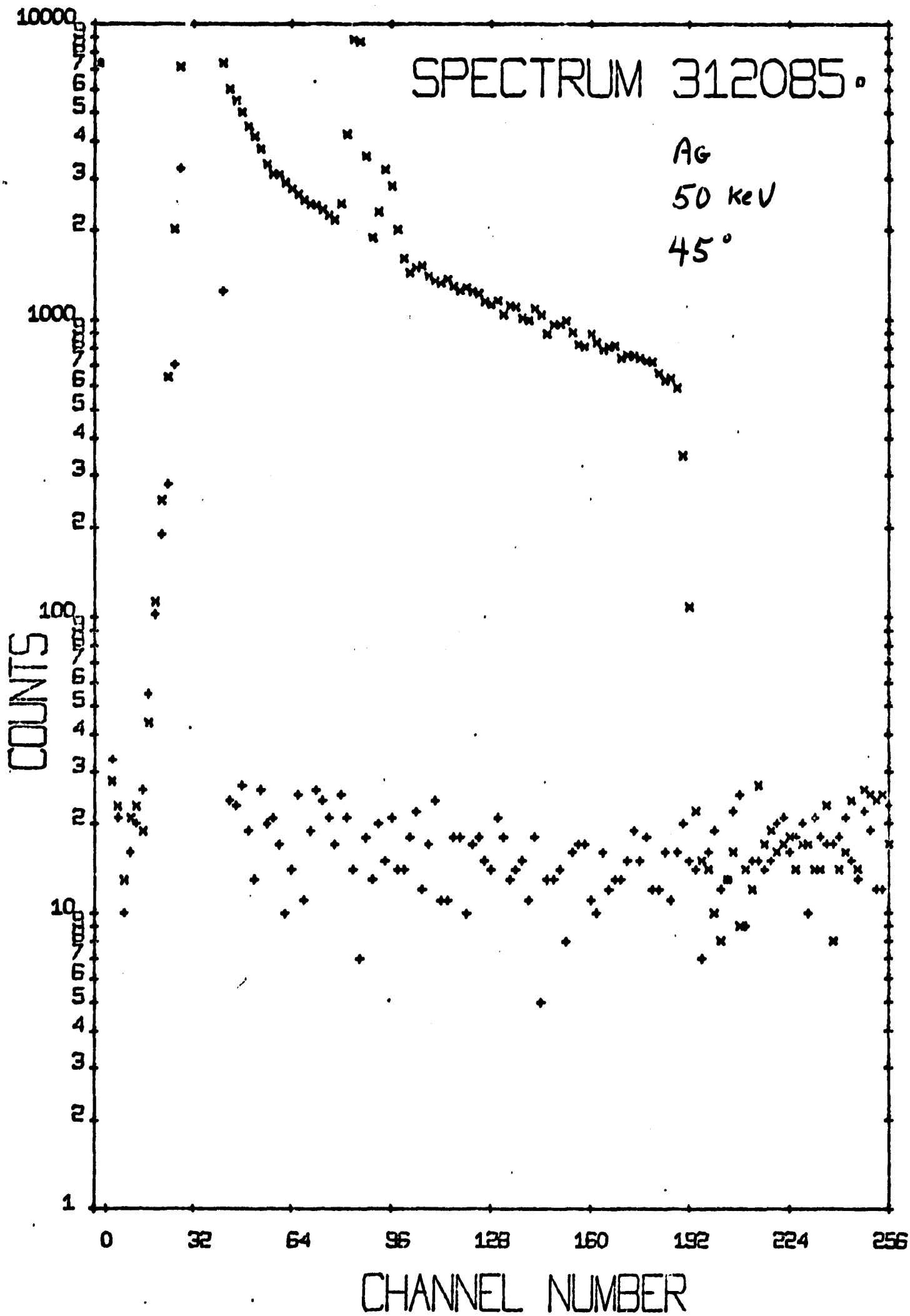


FIG. 14

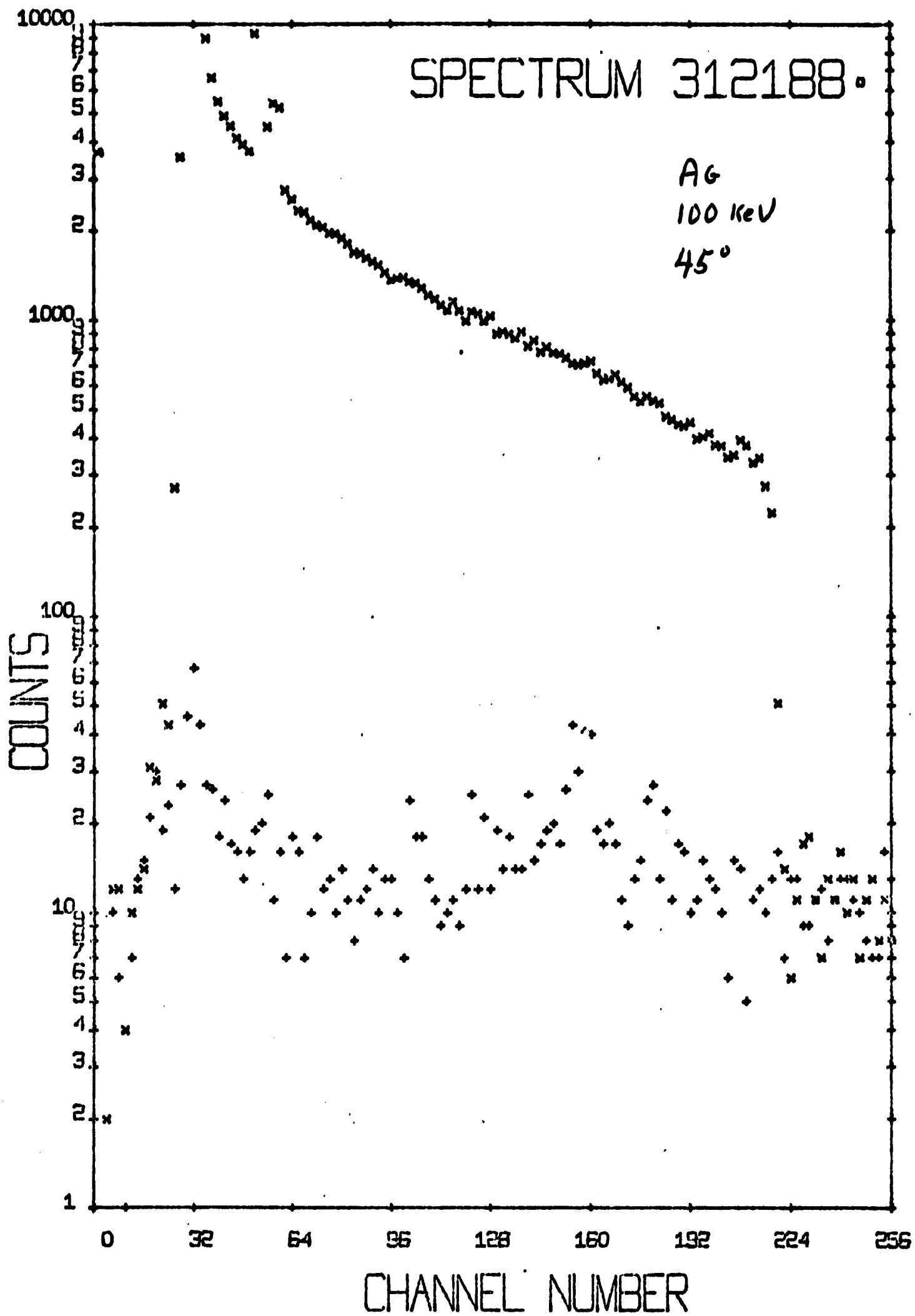


FIG. 15

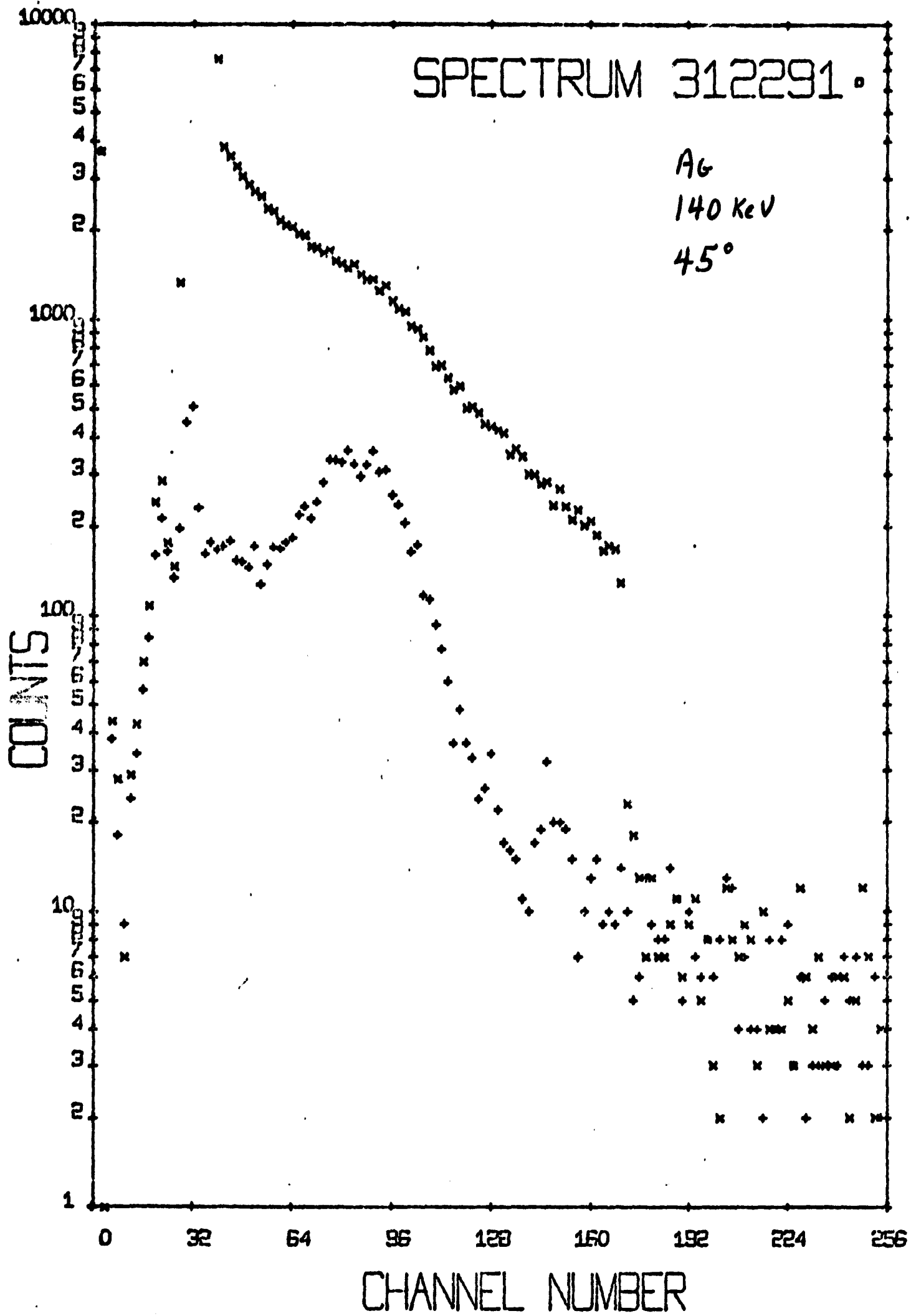


FIG. 16

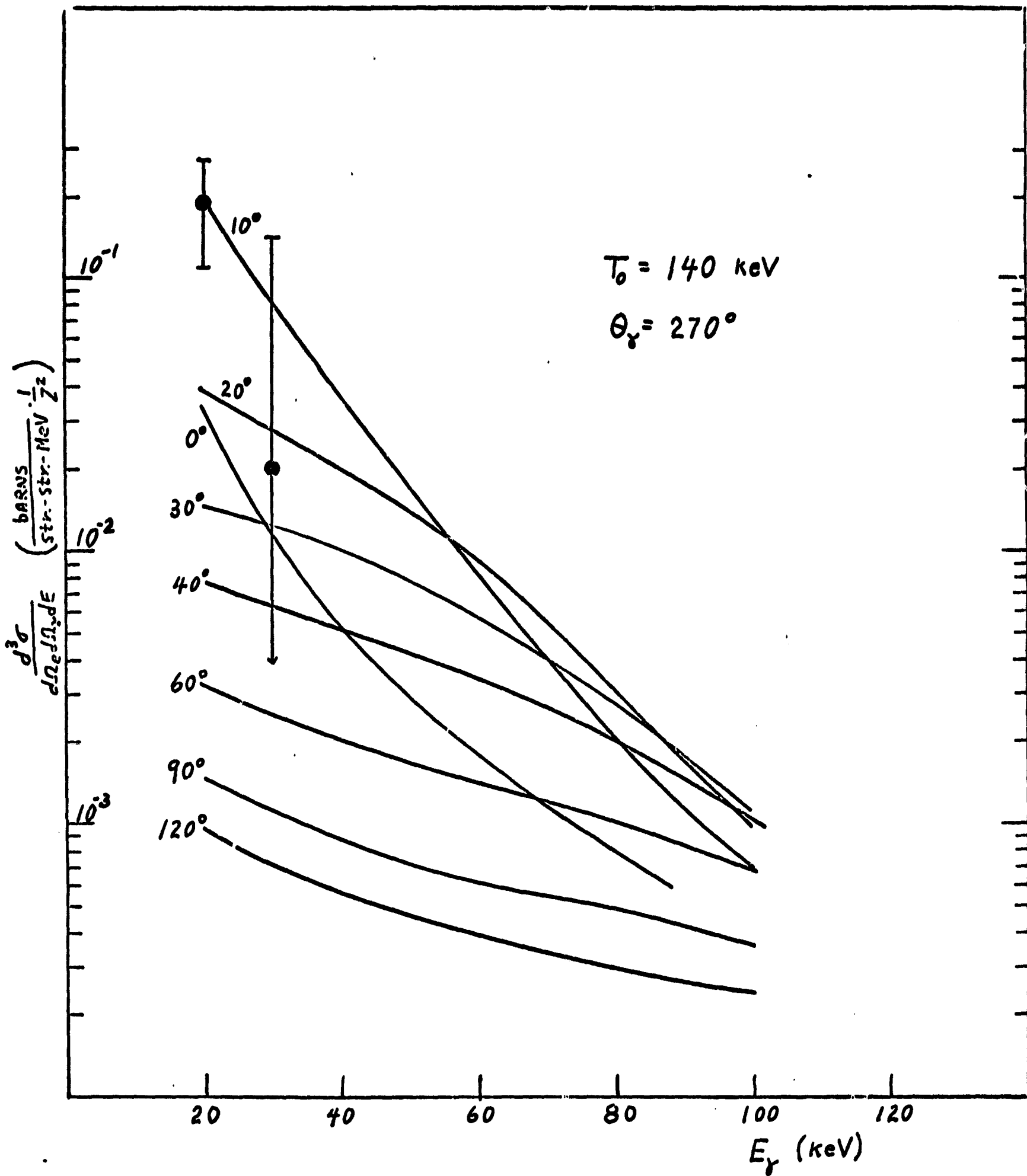


Fig. 17